Articles

Equilibrium Refolding Transitions Driven by Trifluoroethanol and by Guanidine Hydrochloride Dilution Are Similar in GTPase Effector Domain: Implications to Sequence−Self-Association Paradigm†

Jeetender Chugh,‡ Shilpy Sharma,‡ and Ramakrishna V. Hosur*

Department of Chemical Sciences, Tata Institute of Fundamental Research, Homi Bhabha Road, Mumbai-400005, India

Received June 29, 2008; Revised Manuscript Received October 17, 2008

ABSTRACT: Protein folding transitions starting from a denatured state play crucial roles in deciding the final fate of a protein. A fundamental question in this regard is the role of the amino acid sequence of the protein. In this context, we have investigated here the equilibrium refolding to a partially folded state of the GTPase effector domain (GED) of dynamin driven by addition of increasing amounts of trifluoroethanol (TFE) and compared it with that driven by progressive dilution of the guanidine hydrochloride (Gdn-HCl) denaturant, which has been reported recently [Chugh et al. (2008) *Protein Science 17*, 1319−1325]. The structural and dynamics changes as the molecule refolds starting from the Gdn-HCl denatured state have been monitored by circular dichroism, fluorescence, and NMR. The molecule remains a monomer in the TFE limiting case, whereas in the Gdn-HCl case, the molecule self-associates as the denaturant is removed. Even so, the two equilibrium transitions seem to have many similarities. The limiting helical contents are similar, and the regions of progressive increase in millisecond time scale motions, suggestive of slow conformational transitions, are largely the same. Though in the guanidine dilution case the partially folded molecules self-associate and there is multimer−monomer equilibrium, the very high concentration (∼6 M) of guanidine prevents self-association in the case of TFE created species. Taken together, the observations under the drastically different solvation conditions suggest that the GED sequence is designed to self-assemble via helices leading to formation of a fully folded megadalton size assembly. The present observations may also have implications for the folding and association mechanism of the protein. These are important from the point of view of dynamin function.

Protein folding *in vivo* starts from a denatured state. The mechanism by which a protein folds to its fully functional native state, the relation between the sequence and the final structure, the relation between the sequence and the folding pathways, etc., are among the hotly debated questions with no clear answers, one way or the other (*1*−*4*). While there is evidence to say that sequence alone determines the final folded structure, there have been many instances where proteins with very poor sequence homologies have very similar final topologies. Likewise, a given protein under slightly different experimental conditions has been found to adopt completely different conformations; myoglobin, a fully helical protein, forming fibrils under some conditions (*5*) and barstar, an α−*β* protein, forming fibrillar structures (*6*) under some specific conditions are some of the examples. Similarly, there is also an issue as to whether a protein sequence is designed to self-associate, as is required for many biological functions. Such questions can be addressed by studying folding and self-association of different proteins under different experimental conditions.

The classical view of protein folding supports the folding process occurring via defined pathways with structured intermediates (*7*−*11*). A more recent integrated view describes the folding process in terms of a folding funnel, the broad end (top) of which represents the most heterogeneous unfolded state and the narrow bottom of which represents the well-defined folded state. Every member of the ensemble can, in principle, follow an independent folding pathway, but it is also quite likely that a multitude of unstable/unstructured conformations coalesce into a smaller population of partly folded conformations that finally proceed through a few defined intermediates into the final folded state (*12*).

† We thank the Government of India for providing financial support to the National Facility of High Field NMR at the Tata Institute of Fundamental Research, India. J.C. is the recipient of TIFR Alumni Association fellowship for career development through the years 2002−2005.

* Corresponding author. E-mail: hosur@tifr.res.in. Phone: +91-22-22782271, +91-22-22782488. Fax: +91-22-22804610.

‡ These authors contributed equally.

[1] Abbereviations: GED, GTPase effector domain; CD, circular dichroism; HSQC, heteronuclear single quantum coherence; Gdn-HCl, guanidine hydrochloride; TFE, trifluoroethanol; DOSY, diffusion ordered spectroscopy; CPMG, Carr−Purcell−Meiboom−Gill; R_2, transverse relaxation rate.

10.1021/bi801698q CCC: $40.75
Published on Web 11/12/2008

However, very little is currently known about the residue level details of these processes to learn about the relationship between the sequence and the folding processes. In this background, we have compared here the residue level details about the equilibrium refolding paths created by two distinctly different solvent environments in a protein that is known to self-assemble under native conditions.

The protein under investigation here is the GTPase effector domain (GED)[1] of dynamin, a multidomain protein involved in endocytosis (*13, 14*). GED forms megadalton-sized soluble oligomers (even at micromolar concentrations) under native conditions *in vitro* (*15, 16*). The secondary structure predictions, supported by the circular dichroism (CD) study, suggest that these oligomers consist largely of bundles of helical monomers (*15*) and the helical content is roughly 45%, the remaining being unstructured. The oligomers can, however, be dissociated into monomers, by the use of chemical denaturants. Strong denaturants such as urea and Gdn-HCl remove both tertiary and secondary structural elements, whereas SDS preserves the secondary α-helical structures completely. The strongly denatured state provides the ideal initial condition for the folding studies. Starting from a 6 M Gdn-HCl denatured state, we induced refolding by addition of increasing amounts of trifluoroethanol (TFE), a known helix-inducing agent (*17, 18*), and the stepwise formation of structure has been compared with that reported recently (*16*) where refolding was induced by dilution of the denaturant. Clearly, both these represent very different solvation conditions for the protein and the polypeptide chain may be expected to have different preferences in the ensemble as it folds down the funnel. However, strikingly, the equilibrium transitions are found to have many similarities.

EXPERIMENTAL PROCEDURES

Protein Expression and Purification. Recombinant GED was expressed and purified as described earlier (*19*).

Circular Dichroism. Far-UV CD spectra were recorded at 27 °C on a JASCO J-810 spectropolarimeter (Jasco, Europe) using 1 nm bandwidth. All experiments were recorded using 15 μM protein in a fused quartz cell with a path length of 1 mm. Scans were acquired from 215 to 250 nm with a scan speed of 50 nm/min. Each spectrum was an average of 8 scans. The protein samples were equilibrated with different concentrations of TFE, with and without 6 M Gdn-HCl, at least 12 h before recording the experiment. The denaturation profiles were measured at 1%, 2%, 5%, 10%, and 15% TFE concentrations initially and thereafter at an interval of 10% between 20% and 50% TFE. At the end of these experiments, the CD spectra were rerecorded for a few concentrations. These spectra were found to be unaltered, thereby indicating that the samples had acquired equilibrium before acquisition. All the measurements were repeated three times with freshly prepared samples on different days to check for the reproducibility of the profiles. All spectra were baseline corrected by recording the blanks with different concentrations of TFE (with and without 6 M Gdn-HCl) and subtracting these values from that of the protein recorded under identical conditions. The data, thus obtained, were smoothened by three-point averaging to minimize errors due to denaturant concentration adjustments. All the TFE concentrations mentioned in the text throughout are v/v. Near-UV CD spectra (250−300 nm) were recorded with protein concentration of 200 μM under similar conditions as in the case of far UV spectra.

Fluorescence Spectroscopy. Tyrosine steady-state fluorescence was monitored as a function of TFE concentration at constant guanidine concentration (~6 M), at 27 °C with λ_{exc} = 295 nm on a Spex Fluorolog-dM3000f spectrofluorimeter using a 1 cm path length cuvette with a band-pass of 1.5 nm for both excitation and emission. The emission spectra were measured from 300 to 400 nm at a scan rate of 1 nm/s. Protein samples (20 μM) were pre-equilibrated with 6 M Gdn-HCl containing varying amounts of TFE for at least 12 h before the start of the experiment.

4,4′-Bis(1-anilinonaphthalene 8-sulfonate) (bis-ANS) solution was prepared, and the concentration was measured using the extinction coefficient ε_{360} = 23 000 cm^{-1} M^{-1}. Steady-state fluorescence was then measured from 450 to 550 nm with λ_{exc} = 395 nm. Protein samples (20 μM) were pre-equilibrated with varying amounts of TFE with and without 6 M Gdn-HCl (containing 4 μM bis-ANS) for at least 12 h before the start of the experiment.

NMR Spectroscopy. NMR Sample. For NMR based studies, isotopically rich protein samples (^{15}N, ^{13}C, or both) were prepared using M9 media containing $^{15}NH_4Cl$, ^{13}C-enriched glucose, or both as the sole source of nitrogen and carbon, respectively, as described (*19*) and concentrated to 1 mM concentration. The sample was exchanged with acetate buffer (10 mM acetate, pH 5.0) containing 1 mM EDTA, 150 mM NaCl, 1 mM DTT, and 6 M Gdn-HCl. TFE (10% and 20%) was added to the samples, and these were allowed to attain equilibrium (for 12 h) before the start of the experiment.

NMR Data Acquisition and Processing. All the NMR experiments were recorded on a Bruker Avance spectrometer, operating at ^{1}H frequency of 800 MHz, equipped with triple resonance CryoProbe. The ^{1}H and ^{15}N carrier frequencies were set at 4.69 and 118 ppm, respectively. HSQC spectra were recorded and compared at the start and at the end of the experiments to check the stability of the protein samples. No change was observed in these HSQC spectra indicating that the protein was stable under the experimental conditions and had attained equilibrium prior to the start of the experiment. All experiments were processed and analyzed using Felix (Accelrys Software Inc., San Diego, CA). While the close similarity of the peaks observed in the HSQC spectra under varying TFE concentrations permitted transfer of assignments from one to the other, rare ambiguities due to closeness of peaks were resolved by spin-system identification from TOCSY−HSQC (*20*) spectra. All relaxation experiments were carried out using the pulse sequences as described earlier (*21*). ^{15}N transverse relaxation rates (R_2) were measured using CPMG delays of 10, 30, 50*, 90, 130, 170*, 230, and 300 ms, where asterisks indicate points recorded in duplicate for standard error calculations. 2D-DOSY experiments were carried out with a linear gradient of 24 steps between 2% and 95%, a diffusion time of 1000 ms, and the length of the square diffusion encoding gradient pulses of 3 ms; 128 scans were recorded for each gradient step. The standard Bruker protocol was used for processing the DOSY data, and the fitting of the diffusion dimension in the 2D-DOSY spectra was achieved using a two-parameter monoexponential fit (Bruker's DOSY macro in Topspin

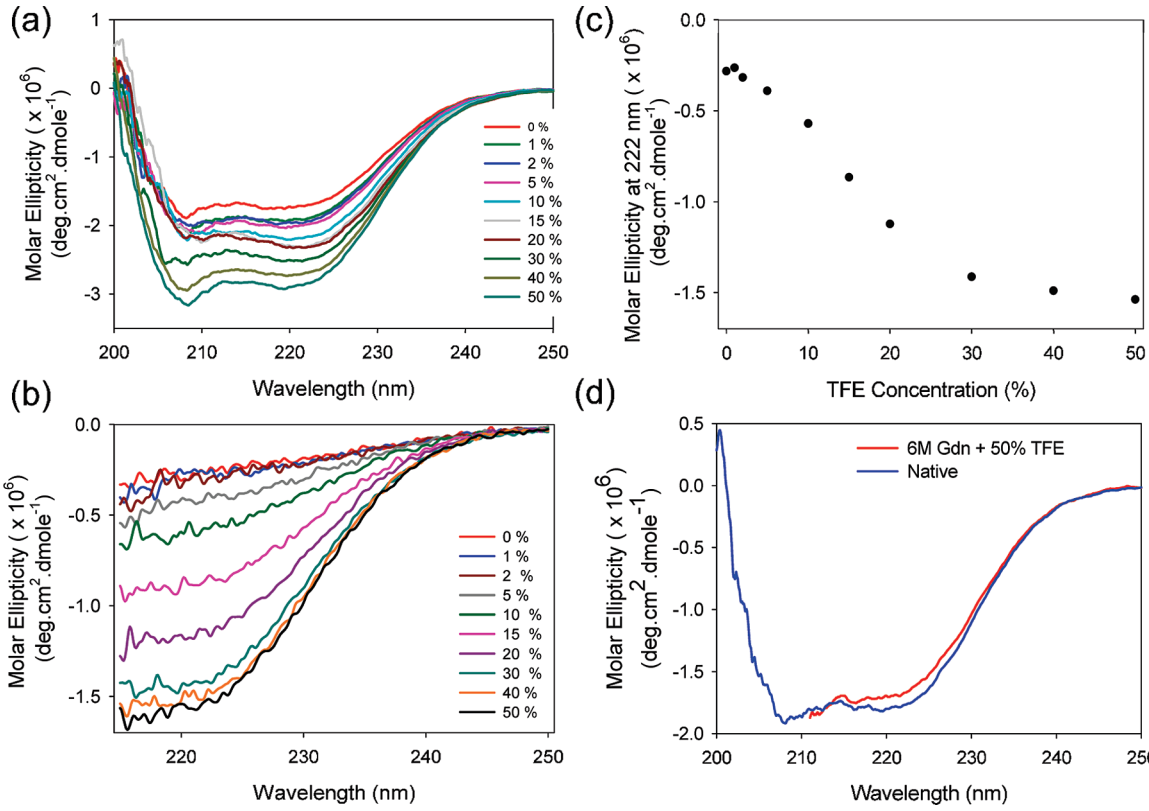

FIGURE 1: Far-UV CD spectra of TFE titration of GED (a) in the absence of guanidine and (b) in ~6 M Gdn-HCl in 20 mM acetate buffer at pH 5.0 containing 1 mM EDTA and 150 mM NaCl, (c) TFE titration as monitored by molar ellipticity at 222 nm and (d) far-UV CD spectra of native-GED (blue) and TFE-driven folded GED (red). The red curve has been truncated below 211 nm since the signal saturated in that region owing to high salt (~6 M Gdn-HCl) concentration.

software). Signals from the methyl regions (1.0−1.2 ppm) were used for the integration.

In all the NMR experiments, ^{1}H chemical shifts were referenced to HDO [4.598 ppm with respect to 2,2-dimethyl-2-silapentane-5-sulfonic acid (DSS) at 15 °C, 6 M Gdn-HCl in acetate buffer, pH 5.0], while the ^{13}C and ^{15}N chemical shifts were indirectly referenced to DSS.

RESULTS AND DISCUSSION

Characteristics of the Initial Gdn-HCl Denatured State. The 6 M Gdn-HCl denatured state, the starting point of the equilibrium refolding exercise undertaken here, has been characterized in detail earlier (*19*). NMR secondary shifts indicated that it displays some residual (ϕ,ψ) preferences along the length of the polypeptide chain and most of these are in the β-region of the Ramachandran map. Besides, NMR relaxation studies showed the presence of four clusters of residues, A (Glu13−Glu26), B (His34−Met66), C (Asn76−Leu90), and D (Met100−Ala123), which displayed differential dynamics along the sequence (*19*).

Folding of GED Driven by Gdn-HCl Dilution. The simultaneous folding and self-assembly of GED as the denaturant concentration is progressively reduced has been described recently (*16*). A combination of different techniques, namely, CD, NMR, DLS, gel filtration etc., was used to derive information on the progressive changes happening in the protein structure and areas susceptible to self-association. A graded disappearance of HSQC peaks toward the middle of the sequence, with a concomitant increase in the helicity (as seen from the far-UV CD spectra), was observed in HSQC-based NMR experiments as the Gdn-HCl concentration was reduced. Furthermore, an enhancement in conformational transitions (millisecond−microsecond time scale) for the residues that were observed in the HSQC spectra also suggested an increased tendency toward structure formation (transient and permanent helices) in these areas on reduction of the denaturant concentration. Thus, using a bottom-up strategy, the residue-wise details of the stepwise folding and concomitant association were recognized (*16*).

TFE-Driven Helix Formation as Monitored by Circular Dichroism and Fluorescence. Taking clues from the Gdn-HCl based experiments that helix formation leads to self-association in GED, we decided to follow an independent pathway wherein increasing amounts of trifluoroethanol (TFE), a helix-inducing agent in peptides, were added to the protein solution in the buffer containing 6 M Gdn-HCl and the structural changes were monitored using CD spectroscopy and tyrosine fluorescence. The changes in molar-ellipticity in far-UV CD spectra reflect the changes in the secondary structure of a protein, while the changes in fluorescence emission reflect the changes in its tertiary structure. The idea was to see how much helicity can be induced (does it span the whole length and make it like a rod) and how does it affect the self-association.

The far-UV CD spectrum of native GED exhibits a characteristic minimum near 222 nm, characteristic of α-helical protein (*16, 19*). The addition of TFE to native GED (i.e., in the absence of guanidine) increases the helicity further (Figure 1a).These full far-UV CD spectra serve as control to show that TFE does indeed induce helicity in GED

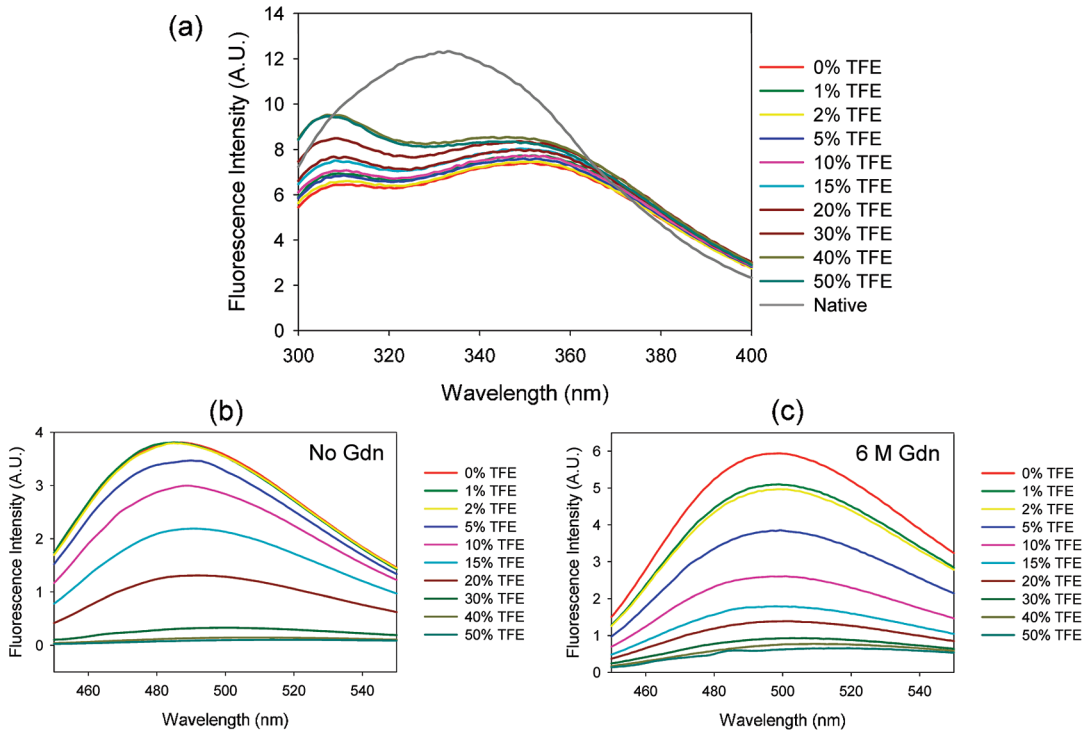

FIGURE 2: (a) Tyrosine fluorescence in GED observed as a function of increasing TFE concentration from 0% to 50% in ~6 M Gdn-HCl in 20 mM acetate buffer at pH 5.0 containing 1 mM EDTA and 150 mM NaCl. The emission spectrum was measured from 300 to 400 nm with λ_{exc} = 295 nm. A protein concentration of 20 μM was used. ANS fluorescence in GED observed as a function of increasing TFE concentration from 0% to 50% (v/v) in (b) the absence and (c) the presence of ~6 M Gdn-HCl. The emission spectra were measured from 450 to 550 nm with λ_{exc} = 395 nm. Fluorescence intensity in each case has been divided by the appropriate excess exponents and is represented in arbitrary units (AU).

and the helicities can be reliably calculated from molar ellipticity at 222 nm ($\theta_{222\,nm}$).

As can be seen from Figure 1b, Gdn-HCl-denatured GED in the absence of TFE (i.e., 0% TFE) does not have significant absorption at 222 nm. However, as the concentration of TFE is increased from 0% to 30%, an increase in the molar ellipticity is observed at 222 nm ($\theta_{222\,nm}$) along with changes in the shape of the spectra consistent with an increase in the helical content (0% at 0% TFE; 10.8% at 10% TFE; 17.7% at 20% TFE, and 23.8% at 30% TFE). Figure 1c depicts the changes in three-point averaged molar ellipticity at 222 nm ($\theta_{222\,nm}$) with gradually varying concentration of TFE. It is observed that very minor changes occur at $\theta_{222\,nm}$ and in the overall CD spectra as the TFE concentration is further increased from 30% to 50% in 6 M Gdn-HCl-denatured GED. It may be concluded that the overall helicity has reached a limiting value by 50% TFE. Also, the concentration of Gdn-HCl has been maintained at 6 M throughout the TFE titration from 0% to 30%, and on further increase of the TFE concentration, the effective Gdn-HCl concentration drops down to 5.33 M in the presence of 50% TFE. The maximum helicity observed at 50% TFE (in the presence of 5.33 M Gdn-HCl) is 34.6%, which is comparable with the helicity estimated by CD for the GED assembly (39.4%) in the native state (Figure 1d) (*16*). Therefore, it may be concluded that the Gdn-HCl-denatured state of GED acquires helical structures in the presence of increasing concentrations of TFE, and this saturates close to the native value.

We recorded near-UV CD spectra to monitor the tertiary structural changes during TFE titration. However, since the protein does not contain any tryptophan, the spectra had very low signal-to-noise ratio, and this prevented a clear analysis (Figure S1, Supporting Information). Nevertheless, it is interesting to see that the spectrum in 50% TFE + 5.33 M Gdn-HCl is more akin to the native spectrum than to the spectrum in 6 M Gdn-HCl. This may indicate a certain degree of tertiary structure induction by TFE.

The tyrosine fluorescence (a tertiary-structure probe) of native-GED displayed a maximum at 332 nm (gray line, Figure 2a), whereas in the 6 M Gdn-HCl-denatured GED, fluorescence maximum shifted to 352 nm with much decreased intensity (red line, Figure 2a). As the concentration of TFE was increased from 0% to 50% (in the presence of Gdn-HCl), an increase in the tyrosine fluorescence intensity was observed indicating some changes in the tertiary structure upon addition of TFE. This is similar to the conclusion from the near-UV CD spectra discussed above. However, even at 50% TFE, fluorescence intensity remained very low as compared with that of native-GED indicating that the tertiary structural changes are rather very minimal.

Further, bis-ANS binding to the protein was monitored to probe the formation of any collapsed hydrophobic core during TFE titration of the protein in 6 M Gdn-HCl (Figure 2b,c). We observed that ANS fluorescence decreases with increasing addition of TFE both in the native condition (Figure 2b) and in the presence of 6 M Gdn-HCl (Figure 2c), where there is no collapsed structure. Therefore, we conclude that the decrease in ANS fluorescence in the native condition is actually a consequence of change in solvent conditions rather than any loss of hydrophobic core on TFE addition. In fact, when a hydrophobic core is not accessible to ANS, opening of the core and exposure of some hydrophobic patches to the solvent leads to an increased ANS

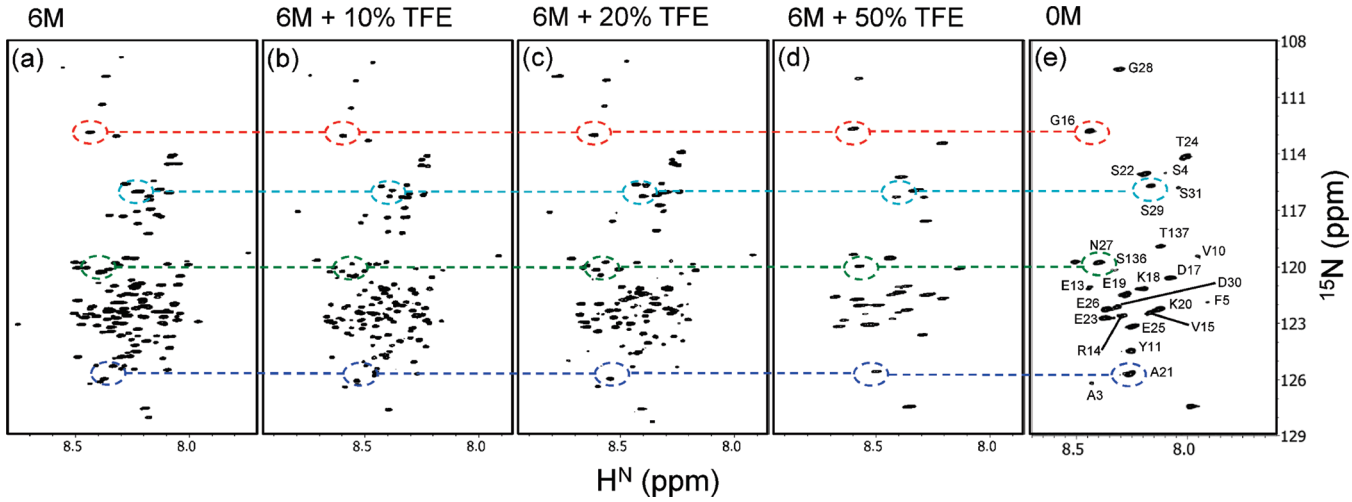

FIGURE 3: $^{1}H-^{15}N$ HSQC spectra of GED in 6 M Gdn-HCl with varying concentrations of TFE: (a) 0% TFE; (b) 10% TFE; (c) 20% TFE; (d) 50% TFE; (e) native GED (in the absence of Gdn-HCl). Dashed circles and lines illustrate the similarity of peak positions, and four representative residues (Gly16, Ser29, Asn27, and Ala21) have been marked for the same; a progressive disappearance of peaks is observed as one proceeds toward the folded state.

fluorescence/binding as has been seen when a transition occurs from a compact fully folded state to a molten globule state (*22*).

NMR Analysis of TFE-Driven Structure Formation. $^{1}H-^{15}N$ HSQC spectrum of GED in its native-like conditions displayed only 26 peaks, as against an expected 132 nonproline peaks (*16*), whereas the number of peaks observed and identified in 6 M Gdn-HCl was 131 (except Glu112) (*19*) (Figure 3a). Upon addition of 10% TFE (keeping guanidine concentration constant at 6 M), the number of peaks reduced to 119 (Figure 3b and Figure S2, Supporting Information). Peak broadening and disappearing from the HSQC spectrum continued with further additions of TFE (69 peaks at 20% TFE and 6 M Gdn-HCl and 25 peaks at 50% TFE and 5.33 M Gdn-HCl; Figure 3c,d). Sequence-specific resonance assignment (shown in Figures S3 and S4, Supporting Information) revealed missing signals in the HSQC spectrum at 20% TFE (Figure S2, Supporting Information) for a continuous stretch between residues Leu65 and Leu87 (except Thr78) (residues between cluster "B" and cluster "C" and of cluster "C") and discontinuous stretch between residues Leu99 and Ile130 (residues of cluster "D"), whereas only the N-terminal 25 residues are seen at 50% TFE (Figure S4, Supporting Information). Peak broadening in the HSQC spectrum upon TFE addition was accompanied with an increase in the helicity as discussed above (Figure 1). The peaks that were visible in the HSQC spectrum of GED at a particular TFE concentration could be correlated in one-to-one fashion with the corresponding peaks at previous TFE concentration or the no TFE (6 M Gdn-HCl) case. Four representative peaks (Gly16, Ser29, Asn27, and Ala21) have been marked in dashed circles and connected with dashed lines, which run across all the HSQC spectra to emphasize this fact (Figure 3); note that the absolute chemical shifts may not be the same because of different solvent conditions. Thus the increase in helicity with increase in TFE concentration could be attributed to the residues that disappeared from the HSQC spectrum. This extensive broadening of the NMR signals beyond detection occurs mainly because of large rotational correlation times in large molecular assemblies or inter/intramolecular conformational exchange. The latter situation is typically seen in molten globules (*23, 24*), which are compact entities where native secondary structures are formed but the tertiary elements are less stable and fluctuate on millisecond−microsecond time scales. It is important to point out here that there is almost a one-to-one correspondence between the peaks in the HSQC spectra of GED in 50% TFE and 5.33 M Gdn-HCl (Figure 3d) and in native-like conditions (Figure 3e); explicit peak assignments in the former case are shown in the Figure S4, Supporting Information. This indicates that at either end-point, the N-termini covering nearly the same stretches remain flexible, and the rest of the sequence participates in structure formation.

Further, to assess the presence of a large mass or molten globule like situation in the final TFE-induced state of GED, we measured the diffusion coefficient using 2D-DOSY experiments (*25*). Pulsed field gradient NMR spectroscopy can be used to measure the translational diffusion coefficient, which reflects the molecular size in solution (*25*). Signals from the methyl regions between 1.0 and 1.2 ppm were used for the integration in DOSY analysis. The integrals measured as a function of the gradient strength (g) were fitted to the following equation:

$$I = I_0 \exp\left[-D\gamma^2 g^2 \delta^2 \left(\Delta - \frac{\delta}{3}\right)\right] \quad (1)$$

where, I is the observed intensity, I_0 the reference or unattenuated intensity, D the diffusion coefficient, γ the gyromagnetic ratio of the observed nucleus, δ the length of the gradient, and Δ the diffusion time. Clearly, the signal decays with increasing g, and a representative decay profile in case of 6 M Gdn-HCl-denatured GED, is shown as a stack plot of the methyl region in Figure 4a; such a profile yields reliable estimates of diffusion constants, and therefore the constants Δ and δ were actually optimized to obtain such a profile. The normalized integral decay profiles for 6 M Gdn-HCl, 6 M Gdn-HCl + 20% TFE, and 6 M Gdn-HCl + 50% TFE as a function of gradient strength are shown in Figure 4b. These upon fitting with eq 1 yielded the following diffusion coefficients: 6 M Gdn-HCl, $(1.352 \pm 0.003) \times 10^{-5}$ cm^2/s; 6 M Gdn-HCl + 20% TFE, $(0.964 \pm 0.001) \times 10^{-5}$ cm^2/s; 6 M Gdn-HCl + 50% TFE, $(0.969 \pm 0.005) \times 10^{-5}$

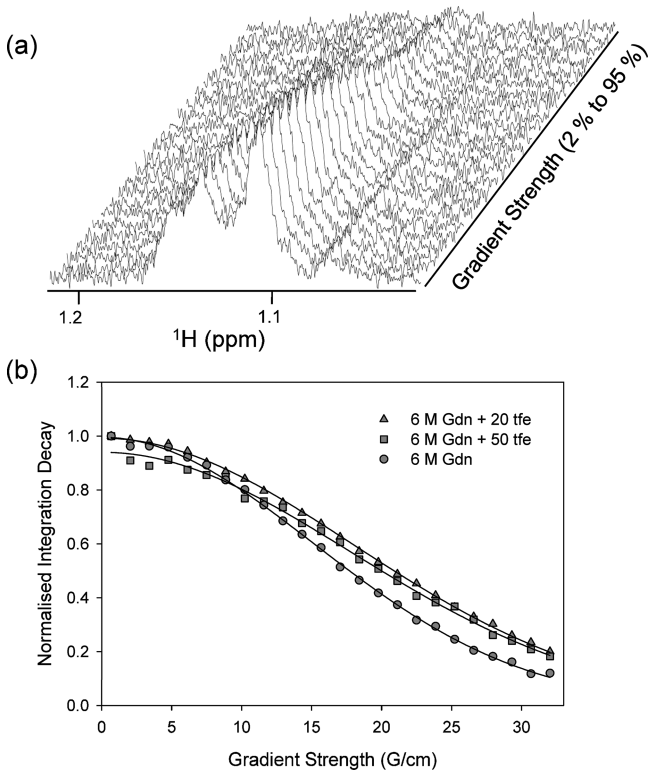

FIGURE 4: (a) Stack plot of representative methyl region (1.0−1.2 ppm) of the 6 M Gdn-HCl-denatured GED as a function of increasing gradient strength from 2% to 95% and (b) normalized integral decay profile of methyl region (1.0−1.2 ppm) for 6 M Gdn-HCl-denatured GED containing 0% (●), 20% (▲), and 50% (■) TFE. The decay has been fitted with eq 1 (see text) to extract the diffusion coefficient in the corresponding solution condition.

cm^2/s. As can be seen, the diffusion coefficients are roughly the same in the three drastically different solvent conditions, which indicates the presence of similar-sized species in solution in all the cases. Since the species in 6 M Gdn-HCl is known to be a monomer, it follows that the dominant population that contributes to the signal in all the DOSY spectra is a monomer. Then, considering that there is no collapsed hydrophobic core in the 50% TFE generated final state, it may be concluded that this species is some kind of an extended structure on an average with well-formed helices and undergoing extensive topological fluctuations on millisecond−microsecond time scale. These motions lead to extensive line broadening to the point of vanishing of peaks in the HSQC spectrum; the N-terminus, which remains as highly flexible as in the native state, behaves like an independent entity and produces HSQC peaks similar to those in the native protein. However, we hasten to add that the existence of a small population of multimeric-GED species can not be totally ruled out since the measurement of diffusion coefficient of such a species would require different optimization of Δ and δ, and thus oligomer and monomer species, if in equilibrium, would not be detected in a single measurement. When the NMR signals from the two overlap, the optimization would reflect only the major species.

The measurement of backbone ^{15}N relaxation rates provides useful insights about the internal molecular dynamics of unfolded and partly folded states. Of these, the transverse relaxation rates (R_2) are largely sensitive to low-frequency motions and act as excellent probes for local conformational transitions that occur on the millisecond to microsecond time scale. A prominent increase in these rates is observed in instances of an increase in such slow conformational exchanges. The residue-wise variation in these relaxation rates can thus be used to monitor the folding transitions as the protein folds from the top to the bottom of the funnel as below.

In the denatured state (top of the funnel), conformational fluctuations will be very rapid. As the chains start making stabilizing contacts as it folds, the motions slow down, and this leads to a progressive increase in the transverse relaxation rates. When the rates reach millisecond time scale, the peaks start to disappear. Thus, by monitoring the progressive increase in the relaxation rates, one can identify the locations of the folding transitions even before the peaks disappear.

In order to investigate the influence of TFE on the conformational dynamics of 6 M Gdn-HCl denatured GED, the residue-wise relaxation parameters were measured in the presence of 10% and 20% TFE and were compared with those of Gdn-HCl-denatured GED. In the guanidine-denatured GED, the relaxation rates showed considerable variation among the 121 residues for which the data was obtained (*19*). The R_2 values ranged from 2.54 ± 0.01 to 8.99 ± 0.02 s^{-1} (average being 5.88 ± 0.21 s^{-1}). From the relaxation analysis, four distinct regions (marked as A Glu13−Glu26, B His34−Met66, C Asn76−Leu90, and D Met100−Ala123) of restricted motion/conformational exchange were identified (*19*). Additionally, the N- and the C-terminal residues showed low R_2 and ^{1}H−^{15}N NOE values (negative values for a few residues, data not shown), indicating increased conformational flexibility in these regions of the polypeptide chain.

Upon addition of 10% TFE to the 6 M Gdn-HCl denatured GED, the relaxation parameters could be determined for 98 residues as opposed to the 121 residues in the denatured state. The difference in the residue-wise R_2 values for the 6 M Gdn-HCl denatured GED in the absence and presence of 10% TFE are shown in Figure 5a. There is an overall increase in the R_2 upon addition of TFE, and part of this increase could be due to increase in the viscosity of the medium (*26*). However, there is also a sequence-wise variation in these changes. Prominent increases (positive changes) in R_2 were observed for the residues in the B, C, and D clusters of residues (marked with solid bars in Figure 5a, top) upon addition of TFE. A special mention needs to be made for residues Ile47, Asp52, Ala56, Asn59, Arg63, and Asp64 (cluster B); Met71−Leu73 (region between clusters B and C); Asn76−Lys79, Glu85, and Leu86 (cluster C); and Glu102−Glu105, Asp111, Leu114, Ala119, and Leu120 (cluster D), which showed an increase of $+3$ s^{-1} in the R_2's in the presence of 10% TFE (Figure 5b). Thus, the increase in helicity (as seen from the CD data) in the guanidine-denatured GED upon addition of 10% TFE is a result of helix formation and conformational exchange in the B, C, and D clusters of residues. All of these are clearly native type in nature, as can be seen by comparison with predicted secondary structural elements shown at the top of the figure.

Further addition of TFE (final concentration 20%) to the 6 M Gdn-HCl-denatured GED led to disappearance of many of those peaks (Asn59, Arg63, Met71−Leu73, Asn76−Asn77, Lys79, Glu85, Leu86, Glu102, Glu105, Asp111, Ala119, and Leu120) for which R_2's had increased at 10% TFE (Figure 3c and Figure S3, Supporting Information) and also led to

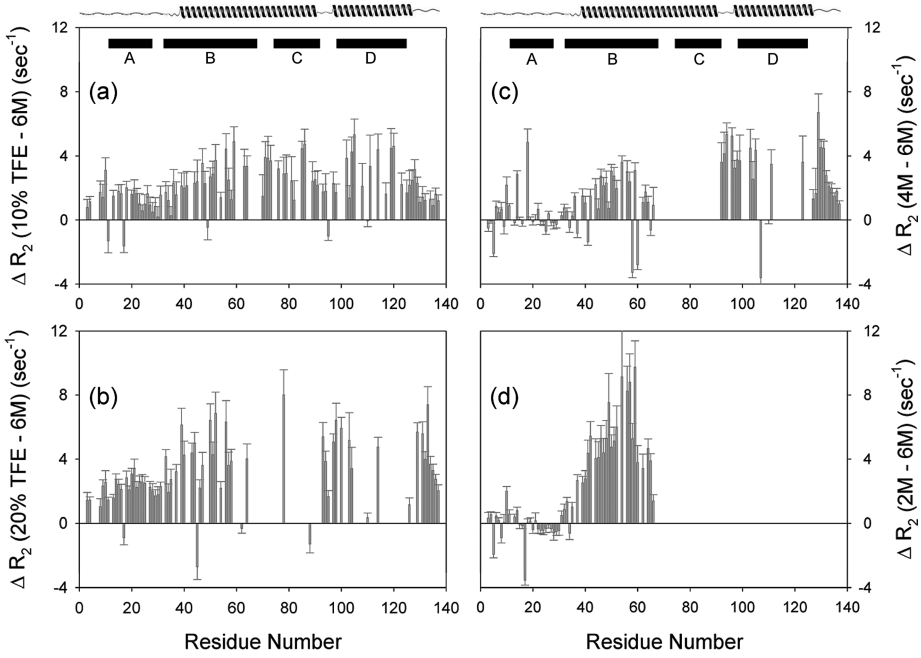

FIGURE 5: The difference in the ^{15}N transverse relaxation rates (R_2) measured (a) in the absence and presence of 10% TFE (with 6 M Gdn-HCl throughout), (b) in the absence and presence of 20% TFE (with 6 M Gdn-HCl throughout), (c) in the presence of 4 and 6 M Gdn-HCl, and (d) in the presence of 2 and 6 M Gdn-HCl. The black bars at the top in panels a and c [marked as A (Glu13−Glu26), B (His34−Met66), C (Asn76−Leu90), and D (Met100−Ala123)], represent areas of significant nonrandom structures (*19*). Predicted secondary structure along the sequence is shown on the top of panels a and c.

increased conformational exchange contributions for many of the residues (Asp52, Ala56, Asp64, Thr78, Ser103, Ala104, and Leu114). The relaxation rate R_2 could be determined for only 68 residues. The differences in the R_2 in the absence and the presence of 20% TFE have been depicted in Figure 5b.

Comparison of TFE Driven and Gdn-HCl Dilution Driven Transitions. We compared the residue-level changes depicting the transitions driven by TFE with similar changes created by Gdn-HCl dilution reported earlier (*16*). For this purpose, the guanidine-dependent relaxation data has been presented in the same manner as for TFE in Figure 5, panel c (difference of residue-wise R_2 values at 4 and 6 M Gdn-HCl) and panel d (difference of residue-wise R_2 values at 2 and 6 M Gdn-HCl). Interestingly, the sequence of changes appears to be very similar in both cases, the same regions getting enhanced R_2's, the same peaks disappearing from the HSQC spectrum, etc. For example, the peaks that have disappeared in Figure 5b are almost the same as those in Figure 5c. There is also some enhancement in the R_2 values in other regions, especially at the N-terminus, in the TFE case. This could be attributed partly to the slowing of conformational fluctuations and partly to enhanced viscosity in 20% TFE; note that addition of TFE increases viscosity and dilution of guanidine decreases viscosity (*26, 27*). The above peaks never broaden out completely, because these are visible even in the final state of the protein reached after addition of 50% TFE (Figure 3d). Thus, the N-terminus remains flexible in the final state reached. The similarities in Figure 5b,c indicate that the condition created at 20% TFE is roughly similar to that created by 4 M Gdn-HCl, so far as the slow conformational transitions are concerned. That is, the formation of helices and the segmental motions occur at almost the same locations along the chain, though from the CD data it appears that the helices are more permanently formed in the TFE case than in the 4 M guanidine case. Thus, not only do the final states reached in the two cases (50% TFE in 5.33 M Gdn-HCl solution and native condition) have many qualitative similarities, as judged from similar HSQC spectra, similar helical contents, and similar near UV CD spectra, but the initial folding transitions (either to 4 M Gdn-HCl or 10% or 20% TFE in presence of 6 M Gdn-HCl) are also similar. In the case of guanidine dilution, the partially folded state self-assembles transiently, whereas the TFE-driven helical state in presence of 6 M Gdn-HCl remains a monomer. The partially folded states in both cases do not possess a rigid tertiary structure or a collapsed hydrophobic core. Only when Gdn-HCl is further diluted, would native like oligomer with hydrophobic core get formed as reflected in intrinsic fluorescence and ANS binding. A summary of the comparison of the two equilibrium-driven transitions described above is depicted in Figure 6.

Sequence−Self-Association Paradigm. We now return to the basic question, to what extent the sequence dictates the self-association property of a given protein. This may not be entirely a fall out of the sequence−structure paradigm, as it is not certain that the molecule has to fold completely to a shape dictated by the sequence for it to start self-associating. The pathways, the stabilities of the species created along the way, and the electrostatic potential surfaces the molecules throw up *vis-a-vis* the solution conditions would play major roles in deciding the final fate of the molecule. Misfolding is one such consequence, and such species are known to aggregate (*28*). In the present case, we started with identical initial conditions for the folding reaction and created two solvation scenarios to force the molecule to move along different paths, as may be dictated by the thermodynamics; the solution environments in the absence and presence of TFE are very different. Furthermore, depletion of Gdn-HCl from the solution in one case changes

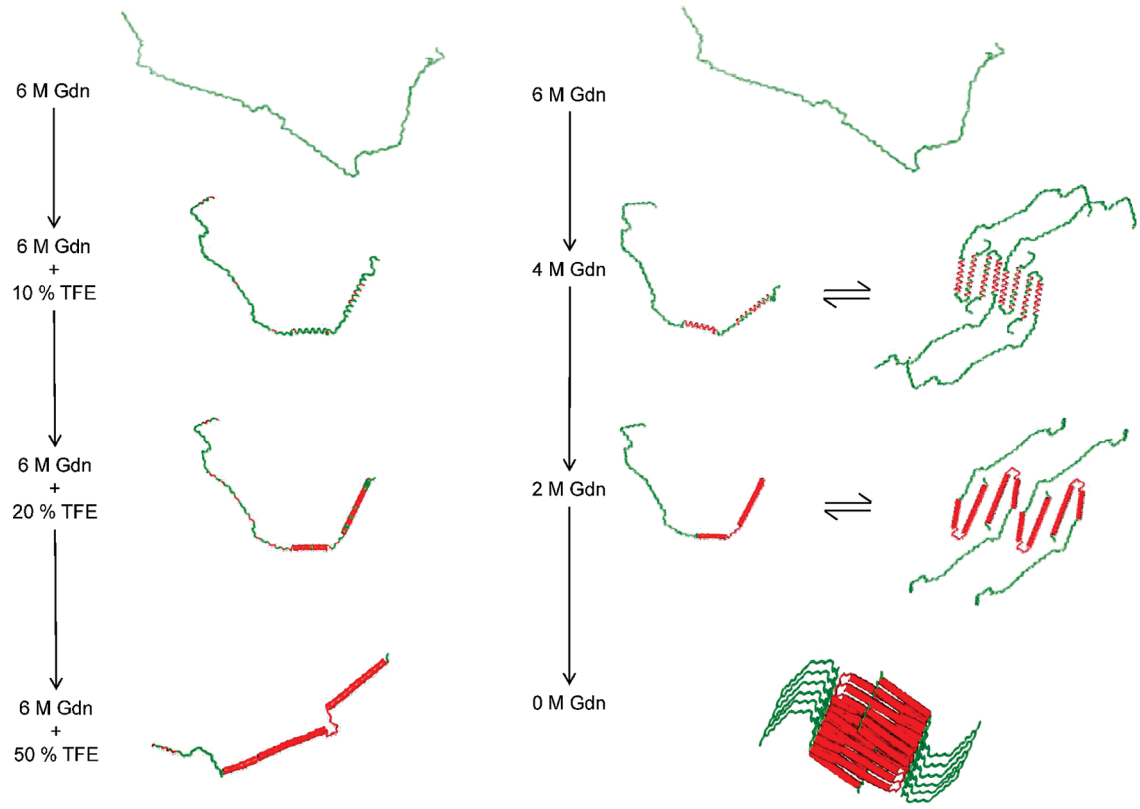

FIGURE 6: Schematic showing the sequence of equilibrium transitions driven by addition of increasing amounts of TFE to denatured GED in 6 M Gdn-HCl (left) and by dilution of Gdn-HCl (right). In the TFE case, the final state is a monomer, whereas in the Gdn-HCl dilution case, the final state is an assembly. In both cases, the secondary structural changes at the intermediate situations occur at similar places along the chain, and the topological fluctuations at millisecond−microsecond time scale also affect the same regions. Red regions in the polypeptide chain correspond to the residues absent in the HSQC in a corresponding solvent condition. To emphasize the difference or similarity in TFE-refolding and Gdn-dilution cases, secondary structural regions (helices and random coil) in the chain have been kept similar. Note that the mode of association shown is only suggestive and not indicative. One can conceive of other modes of association as well. The final point in the TFE-driven case may also have transient intramolecular association, which would contribute to the extensive line broadening seen in the HSQC spectrum.

the ionic strength and also the specific interactions with the protein chain. Despite these drastic differences, it is very interesting to see that the molecule goes through similar folding transitions. The final HSQC spectra and the near-UV CD spectra are similar, though in the TFE case the molecule remains predominantly a monomer because of the high (~6 M) concentration of Gdn-HCl. These indicate that the intramolecular interactions play greater roles in dictating the topologies along the folding pathway, and surfaces highly conducive for self-association are created. In this context, it is also interesting to see that in TFE, a known strongly helix-inducing agent in peptides, the limiting helical content is not very different from that in the native state. This is also similar to what is seen in the monomer created by 2.5% SDS and to what is obtained from secondary structure prediction algorithms, which predict the chain to be helical to about 40−45%. These observations imply that the molecule has an intrinsic property to fold into a topology consisting of certain relative disposition of helices formed, which favors strong intermolecular association, and the solvation differences play only a minor role. In other words, the GED domain is designed to self-assemble, and even partial folding, as is the case at intermediate stages of the folding reaction, can lead to self-association. However, at the intermediate stages, the association may be transient because of lower stability of the assembly compared with the fully assembled state and consequently lower energy barriers for the association−dissociation reaction. These have important consequences for dynamin self-assembly and therefore for its function.

The present observations that the secondary structural transitions are similar in the two drastically different solvation driven scenarios, implying that the sequence has a major role in dictating the folding transitions, may have important implications for the folding mechanism of the protein itself. It may be argued that the sequence of events down the funnel would be intrinsic to the protein. This may mean that so far as the monomer unit is concerned, the end points may have similarities, although in the guanidine-alone case the monomer self-associates and the degree of compactness may not be the same in the two cases; the similarities in the near-UV CD spectra included in the Supporting Information support this view. Further, since the partially folded states are capable of self-associating and considering that structural changes in the associated states are not feasible, we may infer that the intermediates could be on pathway to the folding and self-association process of GED. In other words the equilibrium transitions may also correspond to transitions in a typical kinetic experiment. There can, of course, be many different starting points at the top of the funnel, which can result in many independent folding pathways. If this is true, which we are inclined to believe, detailed structural characterization of the various equilibrium species by NMR and other techniques, which can help probe the core of the

associated state, would throw valuable light on the self-association mechanism of the protein.

ACKNOWLEDGMENT

We thank Dr. Rohit Mittal for the GED clone and Ms. Mamata V. Joshi for the help during the DOSY experiments.

SUPPORTING INFORMATION AVAILABLE

Near-UV CD spectra of GED in native and 6 M Gdn-HCl-denatured (in the presence and absence of 50% TFE) states and the residue specific assignments marked on the $^{1}H-^{15}N$ HSQC spectrum of GED in 6 M Gdn-HCl with 10%, 20%, and 50% TFE concentrations (v/v). This material is available free of charge via the Internet at http://pubs.acs.org.

REFERENCES

1. Brockwell, D. J., Smith, D. A., and Radford, S. E. (2000) Protein folding mechanisms: New methods and emerging ideas. *Curr. Opin. Struct. Biol. 10*, 16–25.
2. Daggett, V., and Fersht, A. R. (2003) Is there a unifying mechanism for protein folding? *Trends Biochem. Sci. 28*, 18–25.
3. Dinner, A. R., Sali, A., Smith, L. J., Dobson, C. M., and Karplus, M. (2000) Understanding protein folding via free-energy surfaces from theory and experiment. *Trends Biochem. Sci. 25*, 331–339.
4. Dyson, H. J., and Wright, P. E. (2004) Unfolded proteins and protein folding studied by NMR. *Chem. Rev. 104*, 3607–3622.
5. Fandrich, M., Forge, V., Buder, K., Kittler, M., Dobson, C. M., and Diekmann, S. (2003) Myoglobin forms amyloid fibrils by association of unfolded polypeptide segments. *Proc. Natl. Acad. Sci. U.S.A. 100*, 15463–15468.
6. Gast, K., Modler, A. J., Damaschun, H., Krober, R., Lutsch, G., Zirwer, D., Golbik, R., and Damaschun, G. (2003) Effect of environmental conditions on aggregation and fibril formation of barstar. *Eur. Biophys. J. 32*, 710–723.
7. Baldwin, R. L. (1989) How does protein folding get started? *Trends Biochem. Sci. 14*, 291–294.
8. Creighton, T. E. (1988) Toward a better understanding of protein folding pathways. *Proc. Natl. Acad. Sci. U.S.A. 85*, 5082–5086.
9. Ptitsyn, O. B. (1991) How does protein synthesis give rise to the 3D-structure? *FEBS Lett. 285*, 176–181.
10. Santucci, R., Sinibaldi, F., and Fiorucci, L. (2008) Protein folding, unfolding and misfolding: Role played by intermediate states. *Mini-Rev. Med. Chem. 8*, 57–62.
11. Wright, P. E., Dyson, H. J., and Lerner, R. A. (1988) Conformation of peptide fragments of proteins in aqueous solution: Implications for initiation of protein folding. *Biochemistry 27*, 7167–7175.
12. Bryngelson, J. D., Onuchic, J. N., Socci, N. D., and Wolynes, P. G. (1995) Funnels, pathways, and the energy landscape of protein folding: A synthesis. *Proteins 21*, 167–195.
13. Hinshaw, J. E. (2000) Dynamin and its role in membrane fission. *Annu. Rev. Cell Dev. Biol. 16*, 483–519.
14. Praefcke, G. J., and McMahon, H. T. (2004) The dynamin superfamily: Universal membrane tubulation and fission molecules? *Nat. Rev. Mol. Cell Biol. 5*, 133–147.
15. Chugh, J., Chatterjee, A., Kumar, A., Mishra, R. K., Mittal, R., and Hosur, R. V. (2006) Structural characterization of the large soluble oligomers of the GTPase effector domain of dynamin. *FEBS J. 273*, 388–397.
16. Chugh, J., Sharma, S., and Hosur, R. V. (2008) NMR insights into a megadalton-sized protein self-assembly, *Protein Sci.*, *17*, 1319–1325.
17. Crandall, Y. M., and Bruch, M. D. (2008) Characterization of the structure and dynamics of mastoparan-X during folding in aqueous TFE by CD and NMR spectroscopy. *Biopolymers 89*, 197–209.
18. Khandelwal, P., Seth, S., and Hosur, R. V. (1999) CD and NMR investigations on trifluoroethanol-induced step-wise folding of helical segment from scorpion neurotoxin. *Eur. J. Biochem. 264*, 468–478.
19. Chugh, J., Sharma, S., and Hosur, R. V. (2007) Pockets of short-range transient order and restricted topological heterogeneity in the guanidine-denatured state ensemble of GED of dynamin. *Biochemistry 46*, 11819–11832.
20. Fesik, S. W., and Zuiderweg, E. R. (1990) Heteronuclear three-dimensional NMR spectroscopy of isotopically labelled biological macromolecules. *Q. Rev. Biophys. 23*, 97–131.
21. Farrow, N. A., Muhandiram, R., Singer, A. U., Pascal, S. M., Kay, C. M., Gish, G., Shoelson, S. E., Pawson, T., Forman-Kay, J. D., and Kay, L. E. (1994) Backbone dynamics of a free and phosphopeptide-complexed Src homology 2 domain studied by 15N NMR relaxation. *Biochemistry 33*, 5984–6003.
22. Goldberg, M. E., Semisotnov, G. V., Friguet, B., Kuwajima, K., Ptitsyn, O. B., and Sugai, S. (1990) An early immunoreactive folding intermediate of the tryptophan synthease beta 2 subunit is a 'molten globule'. *FEBS Lett. 263*, 51–56.
23. Schulman, B. A., Kim, P. S., Dobson, C. M., and Redfield, C. (1997) A residue-specific NMR view of the non-cooperative unfolding of a molten globule. *Nat. Struct. Biol. 4*, 630–634.
24. Wijesinha-Bettoni, R., Dobson, C. M., and Redfield, C. (2001) Comparison of the denaturant-induced unfolding of the bovine and human alpha-lactalbumin molten globules. *J. Mol. Biol. 312*, 261–273.
25. Johnson, C. S., Jr. (1999) Diffusion ordered nuclear magnetic resonance spectroscopy: Principles and applications. *Prog. Nucl. Magn. Reson. Spectrosc. 34*, 203–256.
26. Gente, G., and La Mesa, C. (2000) Water−trifluoroethanol mixtures: Some physicochemical properties. *J. Solution Chem. 29*, 1159–1172.
27. Kawahara, K., and Tanford, C. (1966) Viscosity and density of aqueous solutions of urea and guanidine hydrochloride. *J. Biol. Chem. 241*, 3228–3232.
28. Chiti, F., and Dobson, C. M. (2006) Protein misfolding, functional amyloid, and human disease. *Annu. Rev. Biochem. 75*, 333–366.

BI801698Q